CARBON 68 (2014) 798–806

Available at www.sciencedirect.com

ScienceDirect

journal homepage: www.elsevier.com/locate/carbon

Evaluation and mechanism of antifungal effects of carbon nanomaterials in controlling plant fungal pathogen

Xiuping Wang [a,b], Xueqin Liu [a], Juanni Chen [a], Heyou Han [a,*], Zhaodong Yuan [a]

[a] State Key Laboratory of Agricultural Microbiology, College of Science, Huazhong Agricultural University, Wuhan 430070, PR China
[b] College of Life Science and Technology, Hebei Normal University of Science and Technology, Qinhuangdao 066000, PR China

ARTICLE INFO

Article history:
Received 4 September 2013
Accepted 29 November 2013
Available online 4 December 2013

ABSTRACT

The antifungal activity of six carbon nanomaterials (CNMs, single-walled carbon nanotubes (SWCNTs), multi-walled carbon nanotubes (MWCNTs), graphene oxide (GO), reduced graphene oxide (rGO), fullerene (C_{60}) and activated carbon (AC)) against two important plant pathogenic fungi (*Fusarium graminearum* (*F. graminearum*) and *Fusarium poae* (*F. poae*)) was evaluated. SWCNTs were found to show the strongest antifungal activity, followed by MWCNTs, GO, and rGO, while C_{60} and AC showed no significant antifungal activity. The antifungal mechanism of CNMs was deduced to target the spores in three steps: (i) depositing on the surface of the spores, (ii) inhibiting water uptake and (iii) inducing plasmolysis.

1. Introduction

The plant fungal pathogens *Fusarium graminearum* (*F. graminearum*) and *Fusarium poae* (*F. poae*) are the causative agents of Fusarium head blight (FHB), a global serious plant disease affecting wheat and other cereal (e.g. maize) productions [1,2]. Between 1998 and 2000, direct and secondary economic losses due to FHB for all crops in the Northern Great Plains and Central United States were estimated to be about 3 billion U.S. dollars [3,4]. Furthermore, the *F. graminearum* and *F. poae* not only cause significant losses in crop yield and quality, but also produce mycotoxins that ruin almost all cereals produced in the infected fields [2,5]. Currently, plant cultivars highly resistant to FHB or tolerant of the mycotoxins are not available and the breeding processes are tedious and laborious [6]. Therefore, chemical treatment to these fungi is the main method for plant protection. However, synthetic fungicides are known to be associated with great concerns about risk of fungi resistance, instability, uncontrolled release of anti-infective agent, toxicity to human cells, and eventual depletion of the anti-infective agent [7,8]. In view of limitations in current control measures and the severe impact of FHB on important economical crops, developing alternative agents for effective control of these diseases has become urgent.

Carbon nanomaterials (CNMs) such as graphene oxide (GO) and carbon nanotubes (CNTs) are of particular interest to researchers due to their amazing thermal, mechanical, and electrical properties as well as a wide range of technological applications [9,10]. Recently, the antibacterial activity of CNMs has attracted great attention in the research field [11,12]. Single-walled carbon nanotubes (SWCNTs) and multi-walled carbon nanotubes (MWCNTs) were found to inhibit the growth of gram-negative bacteria and gram-positive bacteria [8], with a minimal cytotoxicity to mammalian cells [12]. One recent study indicated that GO and reduced graphene oxide (rGO) have presented a noticeable cytotoxicity to bacteria but a minimal cytotoxicity to A549 cells [11]. Moreover, we have demonstrated that CNMs such as SWCNTs, MWCNTs, GO and rGO can significantly inhibit the growth of copper-

* *Corresponding author:* Fax: +86 27 87288246.
E-mail address: hyhan@mail.hzau.edu.cn (H. Han).
0008-6223/$ - see front matter
http://dx.doi.org/10.1016/j.carbon.2013.11.072

resistant *Ralstonia solanacearum* [13]. These findings implied that CNMs with superior inhibition ability to bacteria growth can be considered as potential antibacterial agents.

The antifungal effect of CNMs has received only a marginal attention from researchers and few studies have been published in this field [14]. Only one report was published in 2012 about the rGO activity against three fungi, namely *Aspergillus niger* (*A. niger*), *Aspergillus oryzae* (*A. oryzae*) and *Fusarium oxysporum* (*F. oxysporum*) [14]. Moreover, to date, several explorations have been conducted regarding the positive effects of CNMs on host plants [15,16]. Both SWCNTs and MWCNTs are reported to be able to significantly stimulate cell growth and enhance seed germination and plant growth [16,17]. Our previous study also demonstrated positive effects of MWCNTs and GO on the germination and growth of wheat plants [18]. For these reasons, we have been motivated to explore the antifungal properties of CNMs against various pathogenic fungal diseases.

The aim of the current study was to evaluate the antifungal activity of CNMs against two fungi — *F. graminearum* and *F. poae*. First, a comprehensive study was conducted on the antifungal effects of CNMs (SWCNTs, MWCNTs, GO, rGO, C_{60} and AC) on the mycelial growth and spore germination of *F. graminearum* and *F. poae*. Subsequently, *F. graminearum* was used to explore the key factors that may influence the antifungal activity of CNMs. Finally, the direct contact interaction mechanism between CNMs and spores of *F. graminearum*, and ultra-structural changes in the morphology of spores were examined. To the best of our knowledge, this is the first attempt of its kind to address this issue. The experimental results will form the basis of further research about the growth inhibition mechanisms of fungi by CNMs.

2. Experimental

2.1. Carbon nanomaterials

C_{60} (purity: >99.9%) and AC (black powder, purity: >99.5%, moisture content: ⩽10%, suitable for plant cell culture) products were purchased from Sigma–Aldrich. SWCNTs (purity: >99%, OD × length 1–2 nm × 30 μm, –COOH content: 2.83 wt.%), and MWCNTs (purity: >99%, OD × length 8 nm × 30 μm, –COOH content: 3.86 wt.%) were purchased from Shenzhen Nanotech Port Co., Ltd. (China). GO and rGO were prepared as described in the Supporting Information. All suspensions of CNMs were obtained by 30 min sonication using a sonicator bath (Elamsonic, S60H) at 37 kHz less than 550 W without adding any dispersant. The pH values for SWCNTs, MWCNTs, GO, rGO, C_{60} and AC were 6.24, 6.39, 6.46, 7.13, 6.6, and 6.34, respectively. Particle size distributions of CNMs were measured using a Zetasizer Nano ZS90 dynamic light scattering (DLS) system (Malvern, England). Micrographs of CNMs were taken with a digital camera connected to a Leica microscope (Leica, Germany).

2.2. Fungal strains

F. graminearum and *F. poae* were obtained from the State Key Laboratory of Agricultural Microbiology of Huazhong Agricultural University. The fungal cultures were maintained on a potato dextrose agar (PDA) slant at 4 °C. The old cultures were transferred to a fresh slant every 2 months to avoid a decline in strain viability [2].

2.3. Effect of CNMs on mycelial growth of *F. graminearum* and *F. poae*

The antifungal activity on mycelial growth of *F. graminearum* and *F. poae* was tested by following standard procedures as previously reported [19]. Briefly, *F. graminearum* and *F. poae* were inoculated onto solid PDA containing 62.5–500 μg mL^{-1} CNMs or left untreated. After an incubation of 72 h (for *F. graminearum*) and 120 h (for *F. poae*) at 24 ± 2 °C, the mycelial growth and mycelial biomass of pathogenic fungi were observed in each Petri dish. The inhibition percentage of growth (*I*, %) was calculated as follows:

$$I = (1 - dt/dc) \times 100\% \quad (1)$$

where dc is the fungal colony diameter measured in control sets, and dt is the fungal colony diameter measured in treatment sets after 72 h and 120 h of incubation. The antifungal effect was measured under a totally random design with four replicates. The dry weight of mycelia was measured after the mycelial pellets were washed repeatedly with distilled water and dried overnight at 70 °C to a constant weight.

2.4. Spore germination and CNM treatment

For spore germination studies, *F. graminearum* spores were prepared as described previously [20]. Spores incubated in 3% green bean soup liquid medium for 5 days were harvested by centrifugation at 3500 rpm for 5 min and washed twice with sterile distilled water. The spores of *F. poae* fungi were obtained by washing their mycelium with DI water and filtering the resulting suspension through gauze. Both spore suspensions were first adjusted to a concentration of 5×10^5 spores mL^{-1}, and then 80 μL suspensions of spores were mixed with 80 μL of CNMs in the tubes to obtain CNMs at a final concentration of 62.5, 125, 250 and 500 μg mL^{-1}. Control samples containing 80 μL suspensions of spores were mixed with 80 μL DI water. 30 μL mixture with a different concentration of CNMs was transferred onto a concave slide for further incubation at 28 °C for 5 h (for *F. graminearum*) and 12 h (for *F. poae*) in complete darkness. Five concave slides were prepared for each treatment and the mean values were compared. Micrographs were taken with a digital camera connected to a Leica microscope. Spore germination rate (%) was calculated as follows: (the number of germinated spores)/(total number of spores).

2.5. Fluorescence imaging and analysis

The fresh spores were treated with CNMs for 3 h and stained with 4′-6-diamidino-2-phenylindole (DAPI, 3.0 μg mL^{-1}) for 10 min in the dark. Fluorescence images were taken on an Olympus BX40 fluorescence microscope [21].

2.6. Structural and morphological characterization

The spores treated with CNMs for 3 h were fixed with 2.5% glutaraldehyde with a vacuum pump in an ice bath for 30 min, followed by 4 h incubation at 4 °C and three times of

washing with PBS. After that, the spores were postfixed with 1% aqueous OsO_4 (Fluka) for 1 h at 4 °C and washed twice with 0.1 mol/L pH 7.0 phosphate buffers. Subsequently, the spores were dehydrated through ethanol series (30% for 15 min, 50% for 15 min, 70% for 15 min, 90% for 15 min, and 100% for 15 min twice) and embedded in Epon/Araldite resin (polymerization at 65 °C for 15 h). Thin sections (90 nm) were made with an ultra-microtome and stained for 1 min each with 4% uranyl acetate (1:1 acetone/water) and 0.2% Reynolds lead citrate (water), air-dried, and examined under a transmission electron microscopy (TEM, FEI, Czech) [22].

2.7. Determination of spore water content by thermogravimetrical analysis

Thermal gravimetric analysis (TGA) was conducted using a NETZSH TG 209C thermobalance. A minimum of 10 mg of each sample (control spores and spores exposed to CNMs) was heated from room temperature to 200 °C with a heating rate of 5 °C min^{-1} under N_2 and a flow rate of 15 mL min^{-1} [17].

2.8. Statistical analysis

Each treatment was performed in four replicates and arranged in a completely random design. The results are expressed as mean values ± standard deviations (SD). The statistical analysis was performed using the procedure of one-way analysis of variance (ANOVA), and statistical significance was determined by the p value <0.05 (or <0.01). The coefficient of determination (R^2) was calculated to evaluate the relationship between the two values compared.

3. Results and discussion

3.1. Preparation and characterization of GO and rGO

The UV–vis absorption spectroscopy was used to characterize GO and rGO. As shown in Fig. S1A, a maximum occurred at 228 nm in the spectrum obtained form the GO dispersion (attributed to π–π^* transitions of aromatic C=C bonds). After reduction, the maximum red-shifted to approximately 267 nm and the absorption in the whole spectral region (>231 nm) increased, indicating the electronic conjugation had been restored within the graphene nanosheets [23,24].

The structural information of GO before and after being reduced with hydrazine hydrate was investigated using Raman spectroscopy. As shown in Fig. S1B, the characteristic bands for CNMs were D and G bands (1350 and 1580 cm^{-1}), and D/G intensity ratio was assigned to lower defects/disorders in a graphitized structure. Both GO and rGO were observed to be present in the G and D bands, but the intensity ratio (*ID*/*IG*) increased after the GO was reduced with hydrazine hydrate, indicating that a decrease occurred in the average size of the sp^2 domains upon the reduction of the GO [25].

From Fig. S1C, D and E, F, it can be seen that the single-layer GO was around 1 nm thick with smooth appearance and small wrinkles at the edges (Fig. S1D), and rGO aggregated (Fig. S1E and F), which can be attributed to the partial removal of oxygen functional groups on the surface of GO nanosheets during the reduction process [26].

3.2. Dispersibility of CNMs

Aggregation of CNMs exists commonly in aquatic systems [27], and different kinds of aggregation could also significantly influence the interaction between CNMs and fungi. From Fig. S2, a homogeneous solution of SWCNTs, MWCNTs and GO can be observed, indicating that they were well dispersed in water. However, rGO, C_{60} and AC were unable to disperse in water, but rGO showed better dispersity than C_{60} and AC. The size difference in the six aqueous CNMs dispersions was further characterized by DLS. DLS data indicated that the nominal effective diameters of particles in SWCNTs, MWCNTs, GO and rGO were 128, 78.8, 68.06 and 105.7 nm, respectively, while those of C_{60} and AC were 220.6 and 190.1 nm, respectively, suggesting that SWCNTs, MWCNTs, GO and rGO had better dispersibility than both C_{60} and AC. In addition, the light microscopic view of the dispersibility of CNMs shown in Fig. S3 also indicated that SWCNTs, MWCNTs, GO and rGO had better dispersibility than C_{60} and AC, because SWCNTs, MWCNTs, GO and rGO are only a few μm in size, while C_{60} and AC are up to several tens of μm in size.

3.3. Effect of CNMs on mycelial growth of F. graminearum

Hyphae are infection structures to invade plant tissues and the vascular system to cause systemic plant infection [20]. As shown in Fig. S4, SWCNTs, MWCNTs, GO, rGO C_{60} and AC (the data of AC not shown) produced no effect on the mycelial growth rate of *F. graminearum*, but the hyphae density of *F. graminearum* treated by CNMs decreased, which, based on our analyses, can be assumed that the biomass of *F. graminearum* was affected by CNMs. Therefore, the mycelial *F. graminearum* biomass was further measured after being treated with CNMs. As shown in Fig. 1, the biomass of *F. graminearum* hyphae decreased with an increase of CNMs concentration, especially SWCNTs, MWCNTs, GO and rGO, which could significantly reduce the *F. graminearum* biomass, but no significant difference was found in the *F. graminearum* biomass between the treatments of C_{60} and AC and the control. The reason why SWCNTs, MWCNTs, GO and rGO could effectively reduce the mycelial biomass of *F. graminearum* is probably that SWCNTs, MWCNTs, GO and rGO can reduce the branching of fungal hyphae [28]. However, the detailed mechanism by which CNMs affect the branching of fungal hyphae remains to be elucidated.

3.4. Effect of CNMs on spore germination of F. graminearum

Spore germination is an essential developmental stage in the life cycle of all filamentous fungi and represents a preliminary step toward the development of tools that can be further used to characterize early events in the interaction between a pathogen and its hosts [29]. To better understand the functions of CNMs, the antifungal activities of six types of CNMs against *F. graminearum* spore germination were investigated. *F. graminearum* spores (5.0×10^5 spores mL^{-1}) were incubated in dispersions of SWCNTs, MWCNTs, GO, rGO, C_{60} and AC at a concentration range of 62.5–500 μg mL^{-1} for 3 h. A dose-dependent decrease in the percentage of spore germination for the CNMs treated spores is shown in Fig. 2A.

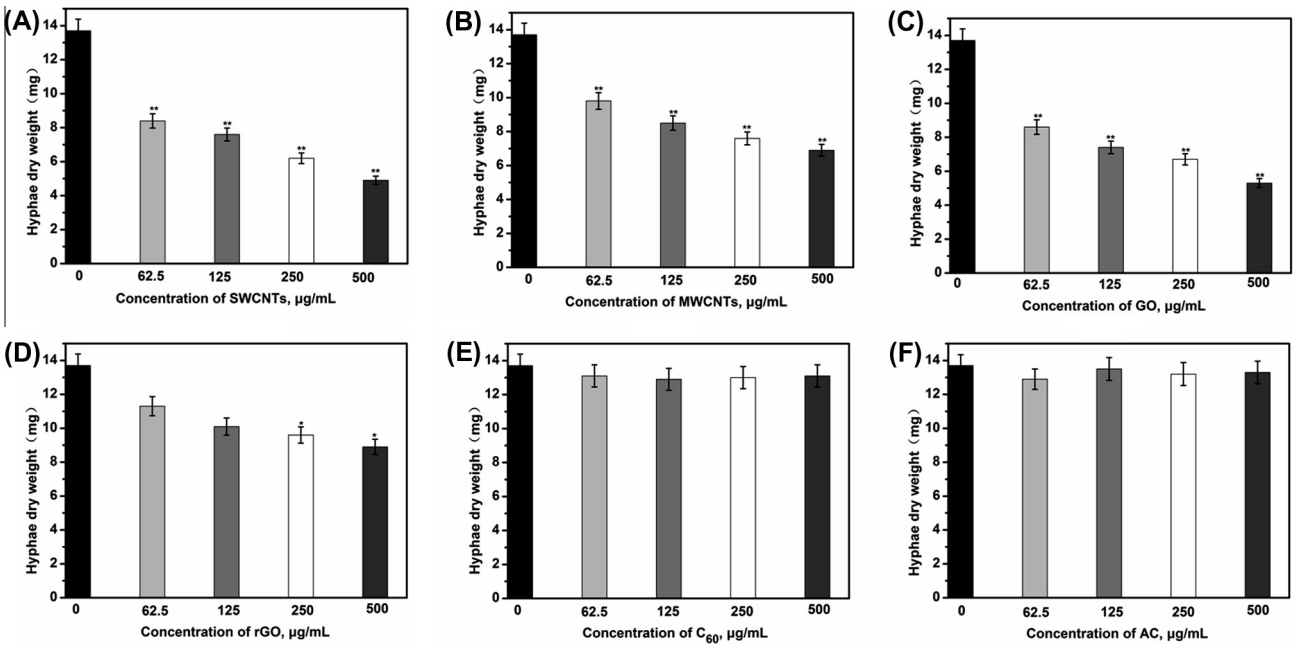

Fig. 1 – Effect of CNMs on the mycelial biomass of *F. graminearum*. Mycelial biomass was tested at different concentrations of (A) SWCNTs, (B) MWCNTs, (C) GO, (D) rGO, (E) C_{60}, and (F) AC dispersions for 72 h at 24 ± 2 °C. Error bars represent the standard deviation (*N* = 4). Where appropriate, statistical significance is indicated: $^{*}p < 0.05$; $^{**}p < 0.01$.

Spores germinated in control conditions (without CNMs) began to form germ tubes after 2 h. At 3 h, 98.1% of the spores possessed germ tubes, while the highest dose of SWCNTs tested (500 μg mL^{-1}) inhibited the germination of spores by >95.2% (Fig. 2Aa). The highest doses of MWCNTs, GO and rGO reduced the germination of spores by about 85.1%, 84.3%, and 50%, respectively (Fig. 2Ab–d). In contrast, at the highest doses of C_{60} and AC, the antifungal activity against *F. graminearum* was significant for C_{60}, but not for AC (Fig. 2Ae and f).

For the sake of visualization, spores were stained with blue fluorescence dye after being mixed with CNMs and then were examined by fluorescence microscopy. As shown in Fig. 2B, SWCNTs, MWCNTs, GO and rGO seemed to be more effective at forming aggregates with the largest involvement of spores, whereas spores on CNM aggregates exhibited a substantial loss of germination viability, while C_{60} was observed to be unable to form spore-C_{60} aggregates, but tend to self-aggregate with the least involvement of spores, indicating that C_{60} cannot exhibit a strong antifungal activity probably because they have fewer chances to mingle with spores. The same phenomenon was also observed in the AC treated spores (data not shown). This result suggests that direct contact between spores and CNMs is essential for the inactivation of spores.

3.5. *Antifungal activity of CNMs against F. poae*

As shown in Fig. 3, CNMs can significantly reduce the mycelial biomass of *F. poae*. From Fig. 3A–D, it can be seen that the mycelial biomass of *F. poae* treated with the highest dose of SWCNTs, MWCNT, GO and rGO (500 μg mL^{-1}) significantly decreased, while the effects of C_{60} and AC on mycelial biomass of *F. poae* showed no significant difference from the control (Fig. 3E and F).

Fig. 4 showed that the effect of CNMs on the spore germination of *F. poae* was dose-dependent. 93.55% of the spores in the control conditions possessed germ tubes after germination, while the germination of spores was inhibited by >90.8% with the highest dose of SWCNTs tested (500 μg mL^{-1}) (Fig. 4A). Meanwhile, the germination of spores was reduced by 84.4%, 82.1%, and 32% with the highest dose of MWCNTs, GO and rGO, respectively (Fig. 4B–D). However, at the highest concentration, C_{60} and AC showed no significant difference from the control in their effects on the spore germination of *F. poae* (Fig. 4E and F).

Fig. S5 displays the representative microscopic images and spores in DI water and the interaction between the spores of *F. poae* and CNMs. As shown in Fig. S5, *F. poae* spores were surrounded and trapped inside significantly by SWCNTs, MWCNTs, GO and rGO. These phenomena are similar to those observed in the CNMs-treated *F. graminearum* in our experiment.

It can be concluded from the above results that CNMs (except for C_{60} and AC) can significantly inhibit the mycelial biomass and spore germination of *F. graminearum* and *F. poae*, and SWCNTs, MWCNTs, GO and rGO have higher antifungal activities than C_{60} and AC. Interestingly, the six types of CNMs are made of pure carbon and only varied from each other in dispersity, which may explain the difference in their antifungal activities against *F. graminearum* and *F. poae*. However, one previous study attributed the difference of antibacterial activity between GO and rGO to their disparity in aggregation/dispersion [30]. To better understand the antifungal mechanism of CNMs, we examined how CNMs interacted with spores using fluorescence microscopy and TEM imaging. The *F. graminearum* spores were chosen as a model to study the interaction

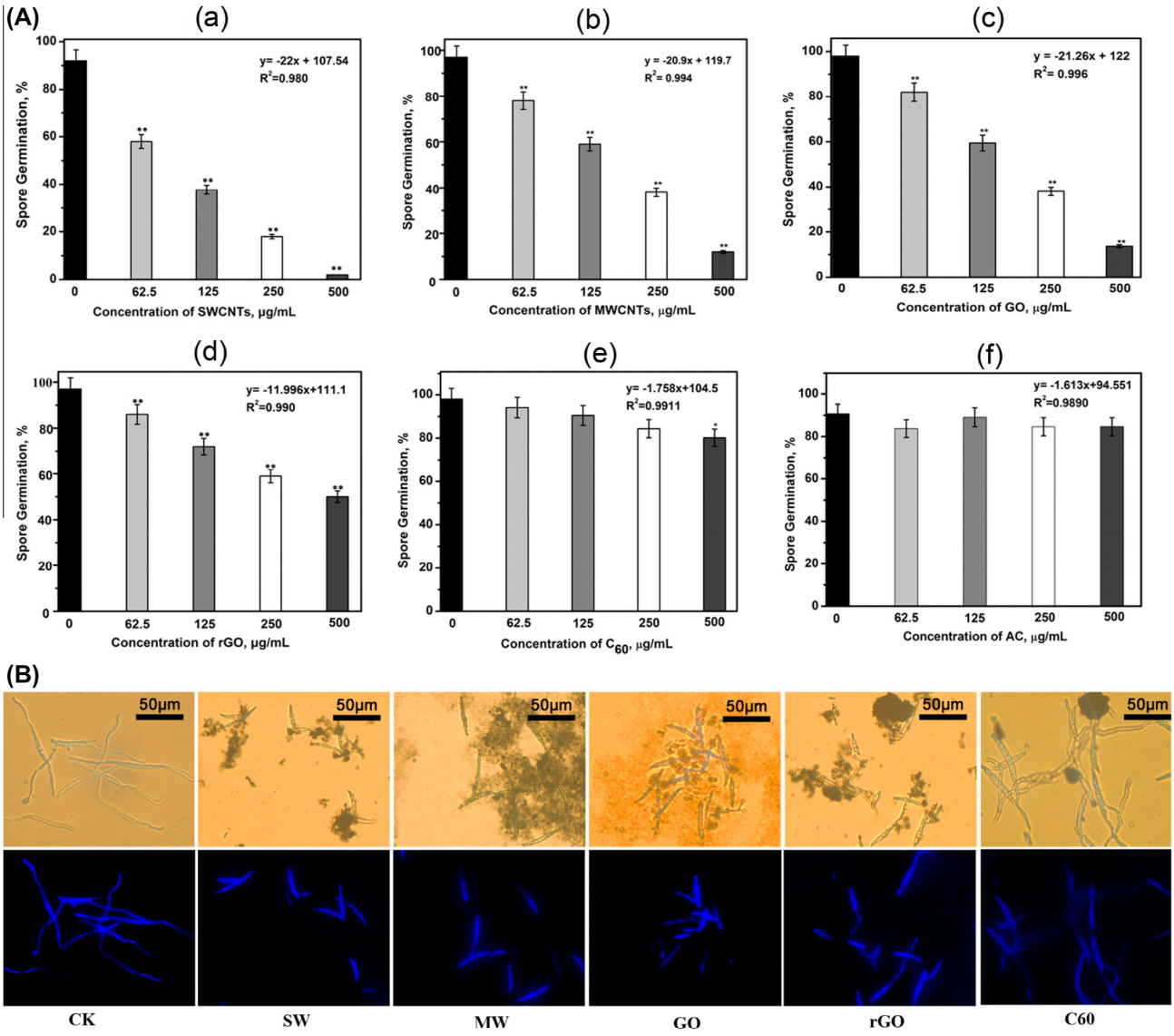

Fig. 2 – (A) Effect of CNMs on spore germination and (B) fluorescence images of *F. graminearum* spores after treatment with CNMs. (A) Spores were germinated on distilled water at 28 °C in darkness at different concentrations of (a) SWCNTs, (b) MWCNTs, (c) GO, (d) rGO, (e) C_{60}, and (f) AC dispersions. Germination was evaluated after 5 h incubation. Error bars represent the standard deviation (N = 4). Where appropriate, statistical significance is indicated: $^{*}p < 0.05$; $^{**}p < 0.01$. (B) The fluorescence images of *F. graminearum* spores after treatment with CNMs. In the upper row is microscopic images of spores treated with and without SWCNTs, MWCNTs, GO, rGO and C_{60}; in the lower row is fluorescence microscope images of spores treated with and without SWCNTs, MWCNTs, GO, rGO and C_{60} (DAPI stained spore). (A colour version of this figure can be viewed online.)

mechanism between CNMs and spores due to their greater germination speed and larger individual size.

3.6. *Mechanism of antifungal activity of CNMs*

3.6.1. *Interaction between CNMs and spores*

Fig. 5 shows the interactions between spores and CNMs obtained by TEM. As shown in Fig. 5B and C, individual SWCNTs and MWCNTs were observed to be interacting with spores, where a few clusters of SWCNTs and MWCNTs were lying beside the spores. In Fig. 5D, the well dispersed GO wrap on spores could be observed and in Fig. 5E, the cluster of rGO could be detected beside the spores. However, due to estranged interaction between spores and C_{60} or AC (data of AC not shown), no C_{60} and AC could be observed around the spores (Fig. 5F). Thus, C_{60} or AC did not exhibit strong antifungal activity probably due to lack of tight or direct contacts with spores. This result also suggests that direct contact between CNMs and spores may play an important role in their antifungal activities, which agrees with a previously published result [21].

Nevertheless, we believe that the aggregation of spores by CNMs is only one of the factors governing their antifungal activity against spores. In this respect, both SWCNTs and

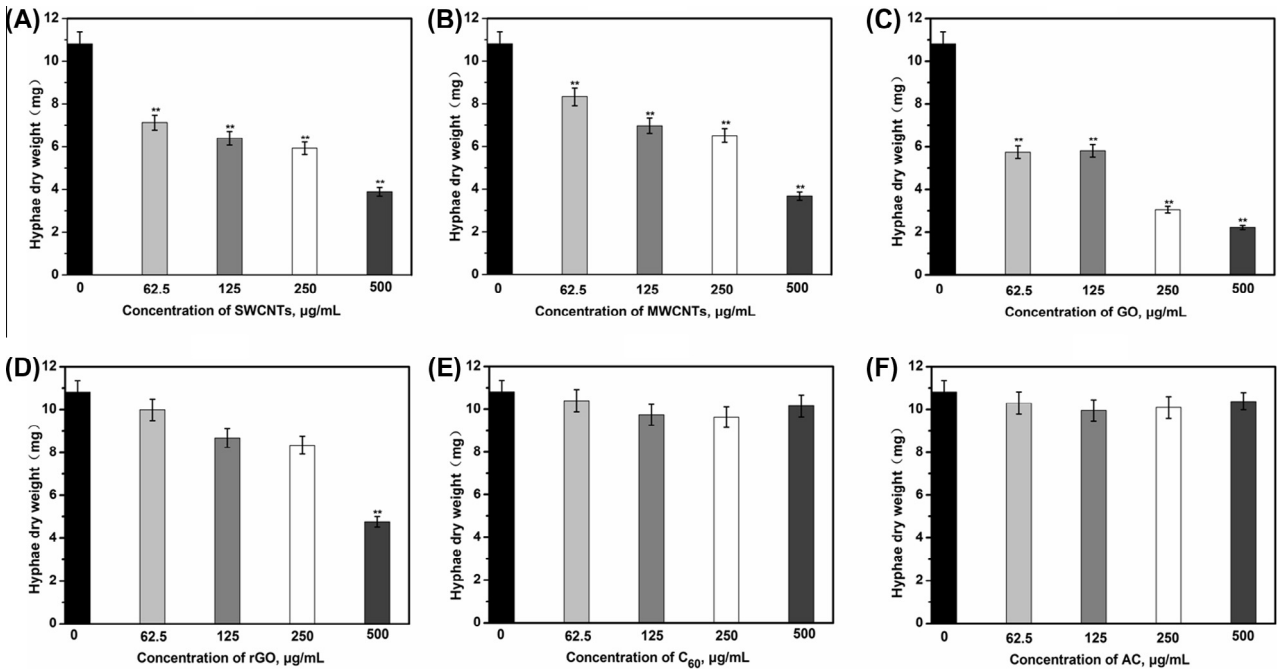

Fig. 3 – Effect of CNMs on the mycelial biomass of *F. poae*. Mycelial biomass was tested at different concentrations of (A) SWCNTs, (B) MWCNTs, (C) GO, (D) rGO, (E) C_{60}, and (F) AC dispersions for 120 h at 24 ± 2 °C. Error bars represent the standard deviation (N = 4). Where appropriate, statistical significance is indicated: $^{*}p < 0.05$; $^{**}p < 0.01$.

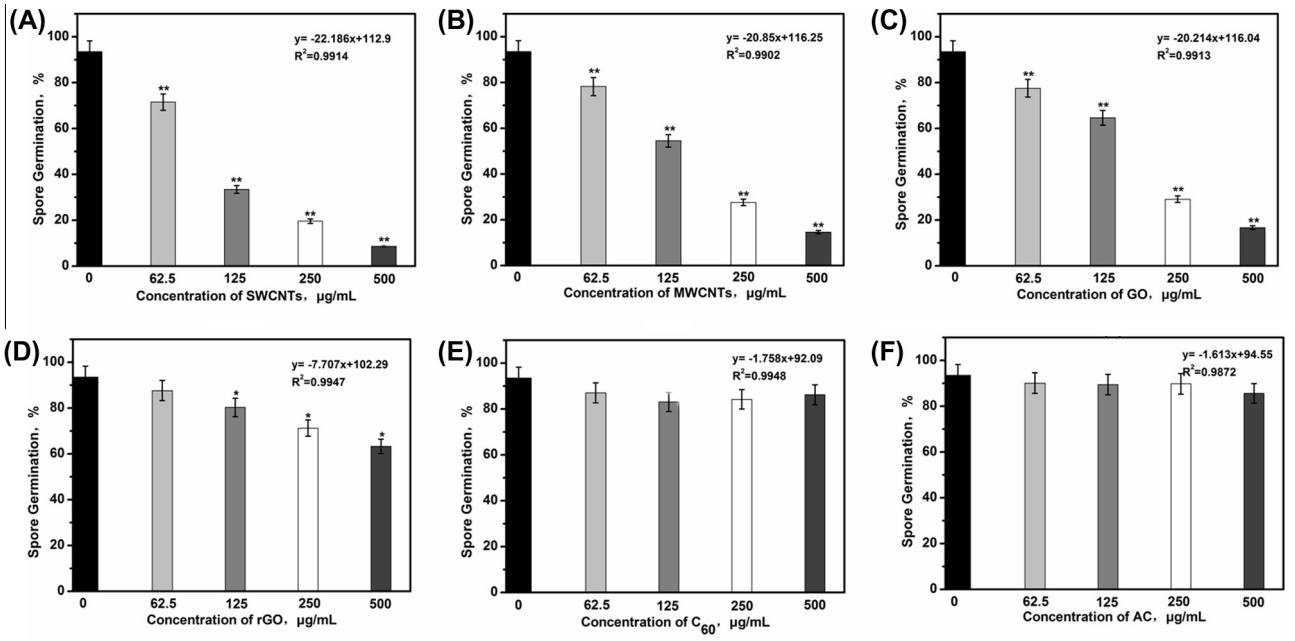

Fig. 4 – Effect of CNMs on spore germination of *F. poae*. Spores were germinated on distilled water at 28 °C in darkness at different concentrations of (A) SWCNTs, (B) MWCNTs, (C) GO, (D) rGO, (E) C_{60}, and (F) AC dispersions. Germination was evaluated after 3 h incubation. Error bars represent the standard deviation (N = 4). Where appropriate, statistical significance is indicated: $^{*}p < 0.05$; $^{**}p < 0.01$.

MWCNTs can interact with, and form the aggregation of spores, but vary from each other in the activity against spores, suggesting that besides direct contact, there may be other factors contributing to the antifungal activity. The van der Waals force between SWCNTs and MWCNTs can be another factor, because it is likely to be a major force governing the formation of the spore-CNT aggregates. As shown in Fig. 6B and C, the Waals force of SWCNTs was strong enough to induce tight contact between the spores and SWCNTs, whereas that of MWCNTs is much weaker to induce loose

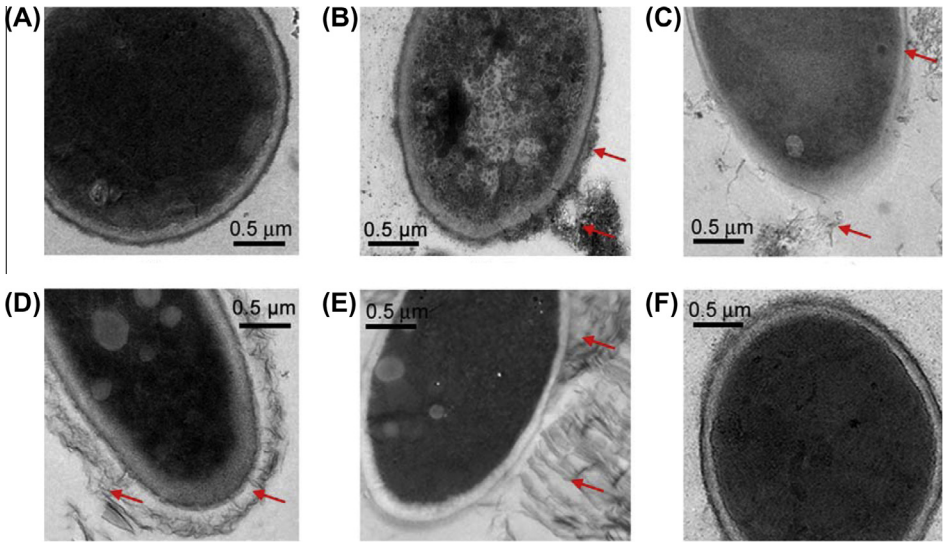

Fig. 5 – TEM images of interactions between *F. graminearum* spores and CNMs. (A) Control spores and (B–F) spores after treatment with SWCNTs, MWCNTs, GO, rGO and C_{60} (at a concentration of 500 μg mL^{-1}). Red arrows indicate CNMs around the spores. (A colour version of this figure can be viewed online.)

contact, resulting in a significant difference in their antifungal activity. This finding is consistent with one previous study [31].

Although GO and rGO can interact with spores, GO has higher fungal inactivation percentage than rGO. Therefore, we believe that the aggregation state of GO and rGO could significantly influence their interaction with spores. One previous study has reported that GO exhibits effective inhibition on *Escherichia coli* growth than rGO, probably due to the marked difference in the dispersion of graphene-based materials [30]. The different behavior of GO and rGO observed in the TEM images also suggested that the well-dispersed, single-atom-thick GO had more chance to contact with spores than rGO, thus generating an effective antifungal activity.

Thus, it can be concluded here that the contact is a key factor for the antifungal activity of CNMs, determining whether CNMs can perform their antifungal functions, but the physical properties of CNMs, such as the Waals force and dispersion state, may determine their antifungal efficiency against spores.

3.6.2. *CNMs can induce plasmolysis of* ***F. graminearum*** **spores**

To find out how CNMs (SWCNTs, MWCNTs, GO and rGO) inhibit the germination of spores, TEM images were used to illustrate ultra-structure changes of spores in response to the CNM action. As shown in Fig. 6A, the healthy cell membrane of *F. graminearum* spores was typically intact and slick; the cell structure was compact and inerratic; and the cytoplasm was well-proportioned. In contrast, the configuration of *F. graminearum* spores after 3 h incubation with CNMs was transfigured and the cytoplasm was no longer well-proportioned but contracted and gathered (Fig. 6B–E). These results provided the evidence of plasmolysis, which can be hypothesized to be related to the water loss of spores induced by CNMs.

It was reported that plasmolysis could be regulated by different stresses such as high osmotic pressure, anoxia, heavy metals, pH, water loss and others [32]. Moreover, water is a major factor required for spore germination in the resumption of cellular metabolism and growth. The rate of water inhibition is dependent on the permeability of the spore coat

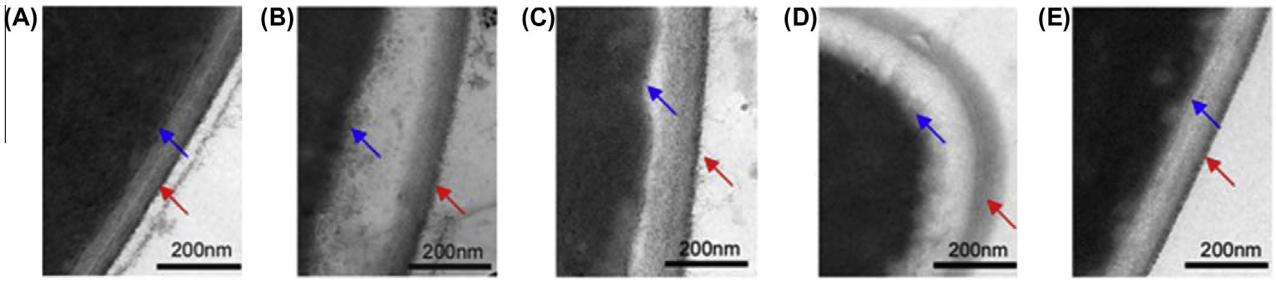

Fig. 6 – Plasmolysis of *F. graminearum* spore induced by CNMs. (A) The spores untreated with CNMs. (B–E) Images of plasmolysis of spores induced by SWCNTs, MWCNTs, GO and rGO after 3 h treatment (at a concentration of 500 μg mL^{-1}), respectively. Blue arrows indicate the cytoplasm; the red arrows indicate cell wall. (A colour version of this figure can be viewed online.)

and the amount of water available in the germination area [29]. Therefore, we hypothesized that the CNMs could inhibit the spore germination just by interfering with the process of water uptake before inducing plasmolysis. This hypothesis could be verified by measuring the water content of spores before and after CNM treatment using thermogravimetric analysis (TGA).

3.6.3. How CNMs inhibit water uptake inside *F. graminearum* spores

To test the aforementioned hypothesis, the moisture level of the spores was examined using TGA. The total level of moisture (%) in the spores was determined by measuring the total mass loss of the spores (Fig. 7A and B). Spores exposed to CNMs were found to possess a significantly lower level of moisture than those untreated with CNMs. Altogether, the moisture detected in the control spores was 61.2%, while moisture levels for the spores exposed to SWCNTs, MWCNTs, GO and rGO were only about 6.6%, 23.8%, 18.9%, and 29.5%, respectively, indicating that CNMs can significantly inhibit the water uptake inside the spores.

The mechanism by which CNMs inhibit water uptake inside the spores is not clear yet. Obviously, the images of the ultra-structure changes of spores indicated that disrupting cell wall by CNMs was not a major cause responsible for the inactivation of spores in this study. It is possible that at high CNM concentrations, water uptake, as well as spore development, could be impeded due to the increased blockage of water channels imposed by surface-adsorbed CNMs. Therefore, the water channel blockage decreased the water content of spores during incubation with CNMs, which could be one factor leading to plasmolysis. Another explanation could be that CNMs were able to regulate the gating of existent water channels (aquaporins) of spores and modify related biological pathways before impacting spore development. It is confirmed that the abnormal expression of several water channel genes, including the important water-channel *LeAqp2* gene in tomato plants, was induced by MWCNTs [33]. However, the spore-specific water channel aquaporins (Aqy1) were shown to be produced during the later stages of sporulation rather than the subsequent maintenance or germination, suggesting that the CNMs cannot regulate the expression of aquaporins [34]. Therefore, water channel blockage imposed by surface-adsorbed CNMs of spores can be speculated to just inhibit the water uptake inside spores, which could be one main factor for plasmolysis and the inhibition of spores' germination, but the detailed mechanism of water channel blockage at proteomic levels induced by CNMs remains to be investigated in future work.

Herein, a general antifungal mechanism of CNMs can be proposed based on the observations in the present work and previous reports on CNM bacterial cytotoxicity. The first step is spore adhesion or deposition onto CNMs, resulting in direct spore-CNM contact during incubation. After the deposition of spores on CNMs, the CNMs may cause the blockage of the water channels of spores. Also, in the antifungal mechanism of CNMs, the plosmolysis of spores could be induced by CNMs.

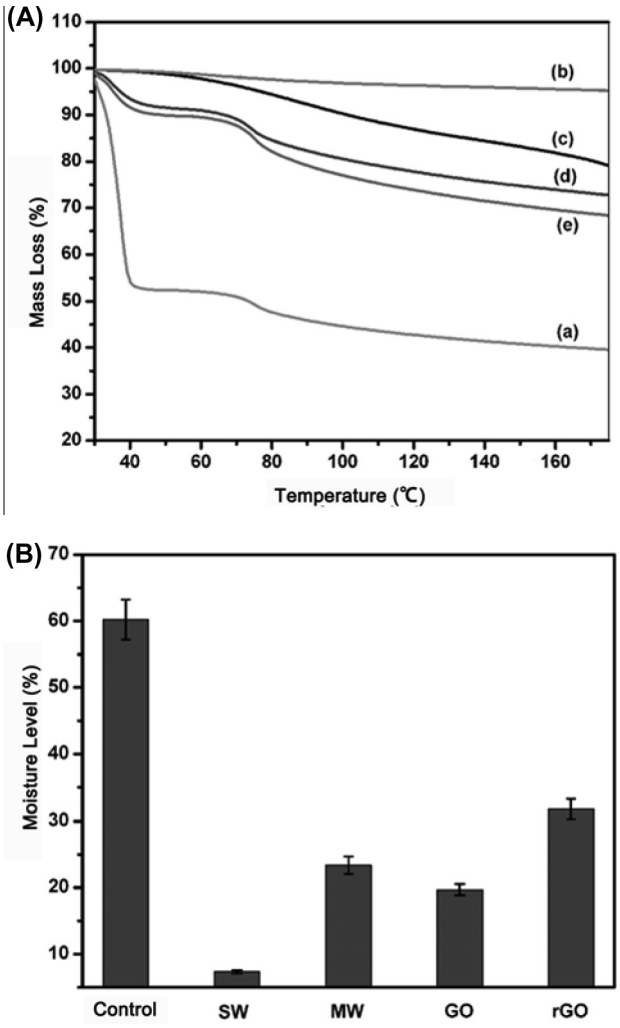

Fig. 7 – (A) Mass loss and (B) moisture levels of *F. graminearum* spores treated with or without CNMs for 3 h. (a) Control spores; (b–e) spores exposed to SWCNTs, MWCNTs, GO and rGO, respectively. (B) Moisture levels of spores incubated with or without SWCNTs, MWCNTs, GO and rGO.

4. Conclusion

This is probably the first report to confirm that CNMs (except for C_{60} and AC) can exhibit strong antifungal activity against *F. graminearum* and *F. poae*. This finding involves two major responses of spores to the action of CNMs: partial or localized plasmolysis due to water loss, and growth arrest. The current study may provide useful information for understanding CNMs as an antifungal agent. Nevertheless, to gain a better understanding of the antifungal mechanism, more plant fungal pathogens should be covered in further laboratory or field studies.

Acknowledgments

The authors gratefully acknowledge the support for this research by National Natural Science Foundation of China

(21175051, 21375043), Fundamental Research Funds for the Central Universities (2012SC04, 2013SC17), Natural Science Foundation of Hubei Province Innovation Team (2011CDA115), and PhD Research Startup Foundation of Hebei Normal University of Science and Technology (2013YB005).

Appendix A. Supplementary data

Supplementary data associated with this article can be found, in the online version, at http://dx.doi.org/10.1016/j.carbon.2013.11.072.

REFERENCES

[1] Chen F, Zhang J, Song X, Yang J, Li H, Tang H, et al. Combined metabonomic and quantitative real-time PCR analyses reveal systems metabolic changes of *Fusarium graminearum* induced by Tri5 gene deletion. Proteome Res 2011;10(5):2273–85.
[2] James WM, Scholastica LM, John MW, Rama DN. Occurrence of *Fusarium* species and associated T2-toxin in Kenyan wheat. Earth Environ Sci 2012;3(1):24–34.
[3] Goswami RS, Xu JR, Trail F, Hilburn K, Kistler HC. Genomic analysis of host–pathogen interaction between *Fusarium graminearum* and wheat during early stages of disease development. Microbiology 2002;152(Pt 6):1877–90.
[4] Rossi1 V, Giosue S, Pattori E, Spanna F, Vecchio AD. A model estimating the risk of Fusarium head blight on wheat. EPPO Bull 2003;33(6):421–5.
[5] Caroline AM, Janet L, Lorien ER, Sanghyun S, Shane JH, Lisa AS, et al. Overexpression of defense response genes in transgenic wheat enhances resistance to Fusarium head blight. Plant Cell 2007;26(4):479–88.
[6] Sintayehu A, Sakhuja PK, Fininsa C, Ahmed S. Management of fusarium basal rot (*Fusarium oxysporum* f. sp. cepae) on shallot through fungicidal bulb treatment. Crop Prot 2011;30(9):560–5.
[7] Semighini CP, Murray N, Harris SD. Inhibition of *Fusarium graminearum* growth and development by farnesol. FEMS Microbiol Lett 2008;279(2):259–64.
[8] Seong KY, Zhao X, Xu JR, Guldener U, Kistler HC. Conidial germination in the filamentous fungus *Fusarium graminearum*. Fungal Genet Biol 2008;45(4):389–99.
[9] Lu FS, Gu LR, Meziani MJ, Wang X, Luo PG, Veca LM, et al. Advances in bioapplications of carbon nanotubes. Adv Mater 2009;21(2):139–52.
[10] Ruiz ON, Fernando KAS, Wang BJ, Brown NA, Luo PG, Mcnamara ND, et al. Graphene oxide: a nonspecific enhancer of cellular growth. ACS Nano 2011;5(10):8100–7.
[11] Hu W, Peng C, Luo W, Lv M, Li X, Li D, et al. Graphene-based antibacterial paper. ACS Nano 2010;4(7):4317–23.
[12] Liu S, Wei L, Hao L, Fang N, Chang MW, Xu R, et al. Sharper and faster "nano darts" kill more bacteria: a study of antibacterial activity of individually dispersed pristine single-walled carbon nanotube. ACS Nano 2009;3(12):3891–902.
[13] Wang XP, Liu XQ, Han HY. Evaluation of antibacterial effects of carbon nanomaterials against copper-resistant *Ralstonia solanacearum*. Colloids Surf B Biointerfaces 2013;103(1):136–42.
[14] Sawangphruk M, Srimuk P, Chiochan P, Sangsri T, Siwayaprahm P. Synthesis and antifungal activity of reduced graphene oxide nanosheets. Carbon 2012;50(14):5156–61.
[15] Khodakovskaya MV, Silva K, Biris AS, Dervishi E, Villagarcia H. Carbon nanotubes induce growth enhancement of tobacco cells. ACS Nano 2012;6(3):2128–35.
[16] Tripathi S, Sonkar SK, Sarkar S. Growth stimulation of gram (*Cicer arietinum*) plant by water soluble carbon nanotubes. Nanoscale 2011;3(3):1176–81.
[17] Khodakovskaya M, Dervishi E, Mahmood M, Xu Y, Li Z, Watanabe F, et al. Carbon nanotubes are able to penetrate plant seed coat and dramatically affect seed germination and plant growth. ACS Nano 2009;3(10):3221–7.
[18] Wang XP, Liu XQ, Han HY, Gu XX, Chen K, Lu DL. Multi-walled carbon nanotubes can enhance root elongation of wheat (*Triticum aestivum*) plants. J Nanopart Res 2012;14(6):841–50.
[19] Haouala R, Hawala S, El-Ayeb A, Khanfir R, Boughanmi NJ. Aqueous and organic extracts of *Trigonella foenum-graecum* L. inhibit the mycelia growth of fungi. J Environ Sci-China 2008;20(12):1453–7.
[20] Seong KY, Zhao X, Xu JR, Güldener U, Kistler HC. Conidial germination in the filamentous fungus *Fusarium graminearum*. Fungal Genet Biol 2008;45(4):389–99.
[21] Yang C, Mamouni J, Tang Y, Yang L. Antimicrobial activity of single-walled carbon nanotubes: length effect. Langmuir 2010;26(20):16013–9.
[22] Ismaiel AA, Ghaly MF, El-Naggar AK. Milk Kefir: ultrastructure, antimicrobial activity and efficacy on aflatoxin B1 production by *Aspergillus flavus*. Curr Microbiol 2011;62(5):1602–9.
[23] Paredes J, Villar-Rodil S, Solis-Fernandez P, Martinez-Alonso A, Tascon J. Atomic force and scanning tunneling microscopy imaging of graphene nanosheets derived from graphite oxide. Langmuir 2009;25(10):5957–68.
[24] Zhou Y, Bao QL, Tang LAL, Zhong YL, Loh KP. Hydrothermal dehydration for the "green" reduction of exfoliated graphene oxide to graphene and demonstration of tunable optical limiting properties. Chem Mater 2009;21(13):2950–6.
[25] Tuinstra F, Koenig J. Raman spectrum of graphite. J Compos Mater 1970;53(3):1126–30.
[26] Stankovich S, Dikin DA, Piner RD, Kohlhaas KA, Kleinhammes A, Jia Y, et al. Synthesis of graphene-based nanosheets via chemical reduction of exfoliated graphite oxide. Carbon 2007;45(7):1558–65.
[27] Lin C, Fugetsu B, Su YB, Watari F. Studies on toxicity of multi-walled carbon nanotubes on *Arabidopsis* T87 suspension cells. J Hazard Mater 2009;170(2–3):578–83.
[28] Harris SD. Branching of fungal hyphae: regulation, mechanisms and comparison with other branching systems. Mycologia 2008;100(6):823–32.
[29] Harris SD. Morphogenesis in germinating *Fusarium graminearum* macroconidia. Mycologia 2005;97(4):880–7.
[30] Liu S, Zeng TH, Hofmann M, Burcombe E, Wei J, Jiang R, et al. Antibacterial activity of graphite, graphite oxide, graphene oxide and reduced graphene oxide: membrane and oxidative stress. ACS Nano 2011;5(9):6971–80.
[31] Kang S, Herzberg M, Rodrigues DF, Elimelech M. Antibacterial effects of carbon nanotubes: size does matter! Langmuir 2007;24(13):8670–3.
[32] Tyerman SD, Bohnert HJ, Maurel C, Steudle E, Smith JA. Plant aquaporins: their molecular biology, biophysics and significance for plant water relations. J Exp Bot 1999;25(50):1055–71.
[33] Khodakovskaya MV, Silva K, Nedosekin DA, Dervishi E, Biris AS, Shashkov EV, et al. Complex genetic, photothermal, and photoacoustic analysis of nanoparticle–plant interactions. Proc Natl Acad Sci USA 2011;108(3):1028–33.
[34] Sidoux-Walter F, Pettersson N, Hohmann S. The *Saccharomyces cerevisiae* aquaporin Aqy1 is involved in sporulation. Proc Natl Acad Sci USA 2004;101(50):17422–7.